

Modelling the inactivation of viruses from the Coronaviridae family in response to temperature and relative humidity in suspensions or surfaces.

Laurent Guillier, Sandra Martin-Latil, Estelle Chaix, Anne Thébault, Nicole Pavio, Sophie Le Poder, Christophe Batéjat, Fabrice Biot, Lionel Koch, Don Schaffner, et al.

▶ To cite this version:

Laurent Guillier, Sandra Martin-Latil, Estelle Chaix, Anne Thébault, Nicole Pavio, et al.. Modelling the inactivation of viruses from the Coronaviridae family in response to temperature and relative humidity in suspensions or surfaces.. Applied and Environmental Microbiology, 2020, 86 (18), pp.e01244-20. 10.1128/AEM.01244-20. pasteur-02908234

HAL Id: pasteur-02908234 https://pasteur.hal.science/pasteur-02908234v1

Submitted on 13 Aug2020

HAL is a multi-disciplinary open access archive for the deposit and dissemination of scientific research documents, whether they are published or not. The documents may come from teaching and research institutions in France or abroad, or from public or private research centers. L'archive ouverte pluridisciplinaire **HAL**, est destinée au dépôt et à la diffusion de documents scientifiques de niveau recherche, publiés ou non, émanant des établissements d'enseignement et de recherche français ou étrangers, des laboratoires publics ou privés.



Distributed under a Creative Commons Attribution - NonCommercial - NoDerivatives 4.0 International License

- 1 Modelling the inactivation of viruses from the *Coronaviridae* family in response to
- 2 temperature and relative humidity in suspensions or surfaces.
- 3

4 Authors:

- 5 Laurent Guillier,^a Sandra Martin-Latil,^b Estelle Chaix,^a Anne Thébault,^a Nicole Pavio,^c
- 6 Sophie Le Poder,^c on behalf of Covid-19 Emergency Collective Expert Appraisal Group,^d
- 7 Christophe Batéjat,^e Fabrice Biot,^f, Lionel Koch,^f Don Schaffner,^g Moez Sanaa,^a
- 8

9 Affiliations:

- 10 ^aRisk Assessment Department, French Agency for Food, Environmental and
- 11 Occupational Health & Safety, 14, rue Pierre et Marie Curie, Maisons-Alfort, France
- 12 ^bLaboratory for food safety French Agency for Food, Environmental and Occupational
- 13 Health & Safety, University of Paris-EST, Maisons-Alfort, France
- 14 ^cUMR Virologie 1161, ENVA, INRAE, Anses, Maisons-Alfort, France
- ^dMembership of the Covid-19 Emergency Collective Expert Appraisal Group is provided
- 16 in the Acknowledgments
- ¹⁷ ^eEnvironment and Infectious Risks Unit, Laboratory for Urgent Response to Biological
- 18 Threats (CIBU), Institut Pasteur, Paris, France
- 19 ^fBacteriology Unit, French Armed Forces Biomedical Research Institute (IRBA),
- 20 Brétigny-sur-Orge, France
- 21 ^gDepartment of Food Science, Rutgers University, New Brunswick, NJ, USA

22

23 Affiliations:

- 24 Running Head: Modelling the inactivation of coronaviruses on fomites
- 25 #Address correspondence to laurent.guillier@anses.fr

26 Abstract:

27	Temperature and relative humidity are major factors determining virus inactivation in the
28	environment. This article reviews inactivation data of coronaviruses on surfaces and in
29	liquids from published studies and develops secondary models to predict coronaviruses
30	inactivation as a function of temperature and relative humidity. A total of 102 D-values
31	(time to obtain a log_{10} reduction of virus infectivity), including values for SARS-CoV-2,
32	were collected from 26 published studies. The values obtained from the different
33	coronaviruses and studies were found to be generally consistent. Five different models
34	were fitted to the global dataset of D-values. The most appropriate model considered
35	temperature and relative humidity. A spreadsheet predicting the inactivation of
36	coronaviruses and the associated uncertainty is presented and can be used to predict
37	virus inactivation for untested temperatures, time points or any coronavirus strains
38	belonging to Alphacoronavirus and Betacoronavirus genera.
38 39	belonging to <i>Alphacoronavirus</i> and <i>Betacoronavirus</i> genera. Importance: The prediction of the persistence of SARS-CoV-2 on fomites is essential to
39	Importance: The prediction of the persistence of SARS-CoV-2 on fomites is essential to
39 40	Importance : The prediction of the persistence of SARS-CoV-2 on fomites is essential to investigate the importance of contact transmission. This study collects available
39 40 41	Importance : The prediction of the persistence of SARS-CoV-2 on fomites is essential to investigate the importance of contact transmission. This study collects available information on inactivation kinetics of coronaviruses in both solid and liquid fomites and
39 40 41 42	Importance : The prediction of the persistence of SARS-CoV-2 on fomites is essential to investigate the importance of contact transmission. This study collects available information on inactivation kinetics of coronaviruses in both solid and liquid fomites and creates a mathematical model for the impact of temperature and relative humidity on
39 40 41 42 43	Importance: The prediction of the persistence of SARS-CoV-2 on fomites is essential to investigate the importance of contact transmission. This study collects available information on inactivation kinetics of coronaviruses in both solid and liquid fomites and creates a mathematical model for the impact of temperature and relative humidity on virus persistence. The predictions of the model can support more robust decision-
 39 40 41 42 43 44 	Importance: The prediction of the persistence of SARS-CoV-2 on fomites is essential to investigate the importance of contact transmission. This study collects available information on inactivation kinetics of coronaviruses in both solid and liquid fomites and creates a mathematical model for the impact of temperature and relative humidity on virus persistence. The predictions of the model can support more robust decision-making and could be useful in various public health contexts. Having a calculator for the
 39 40 41 42 43 44 45 	Importance: The prediction of the persistence of SARS-CoV-2 on fomites is essential to investigate the importance of contact transmission. This study collects available information on inactivation kinetics of coronaviruses in both solid and liquid fomites and creates a mathematical model for the impact of temperature and relative humidity on virus persistence. The predictions of the model can support more robust decision-making and could be useful in various public health contexts. Having a calculator for the natural clearance of SARS-CoV-2 depending on temperature and relative humidity could

49 **1. Introduction**

50 The pandemic of coronavirus respiratory infectious disease (COVID-19) initiated in 51 Wuhan, China in December 2019 was caused by an emergent virus named Severe 52 Acute Respiratory Syndrome Coronavirus 2 (SARS-CoV-2). SARS-CoV-2 belongs to the 53 order Nidovirales, family Coronaviridae. These enveloped viruses have a positive, 54 single-stranded RNA genome (directly translated) surrounded by a nucleocapsid protein. 55 Coronaviruses are classified into four genera: alpha (α CoV), beta (β CoV), gamma 56 (χ CoV), and delta (δ CoV). SARS-CoV-2 belongs to the *Betacoronavirus* genus and the 57 Sarbecovirus sub-genus. 58 The route of transmission of respiratory viruses is airborne via inhalation of droplets and 59 aerosols or through contact with contaminated intermediate objects (fomites), e.g. by 60 self-inoculation of mucous membranes (mouth, eyes) by contaminated hands (1). The 61 transmission route for SARS-CoV-2, SARS-CoV and Middle East respiratory syndrome 62 (MERS-CoV) is primarily airborne (2-5) while environmental contamination through 63 surfaces is uncertain (6-8). No study has currently quantified the importance of surface 64 contact transmission in the spread of coronavirus diseases (9). Viral genomes have 65 been detected in the stools of COVID-19 patients and sewage (10), but the role of liquid 66 fomites has not yet been addressed. 67 Working with highly virulent coronavirus requires biosafety level 3 laboratory 68 containment conditions and since SARS-CoV2 emerged very recently, few data on its 69 survival related to environmental conditions are available (11, 12). The use of surrogate 70 coronaviruses has been suggested to overcome these challenges and expand the 71 available data on coronavirus survival likelihood (13). Surrogates can be used under the

72	assumption that they have similar physicochemical properties that mimic the viruses
73	they represent (14, 15).
74	Temperature and relative humidity have been shown to impact the kinetics of
75	inactivation of coronaviruses. Increased temperatures have been shown to increase the
76	rate of the inactivation (11, 16), and decreased relative humidity have been associated
77	with a reduction of coronaviruses inactivation rate on surfaces (13, 17-19). Inactivation
78	rates were lower in suspensions compared to surfaces in studies that tested both
79	suspensions and surfaces at similar temperatures (11, 20).
80	Hence, the prediction of the persistence of SARS-CoV-2 on fomites is essential to
81	investigate the importance of contact transmission. This study collects available
82	information on inactivation kinetics of coronaviruses in both solid and liquid fomites and
83	models the impact of temperature and relative humidity on virus persistence.

84

85 2. Materials & methods

86 2.1. Selection of the studies

87 Four inclusion criteria were used to identify studies that characterized inactivation of 88 coronaviruses according to temperature and relative humidity. Selected studies had to 89 focus on one virus from the Coronaviridae family. Inactivation must have been carried out in suspensions or on inert non-porous surfaces. Only surfaces without antimicrobial 90 91 properties were considered. The quantification of infectious viruses had to be assessed 92 by cell culture, since RT-qPCR can underestimate actual virus infectivity (21, 22). 93 Finally, the available kinetics data points should be sufficient to allow precise statistical 94 estimation of the rate of viral inactivation without bias. In this context, kinetic data with

- 95 no significant inactivation observed during the experiment or with values below the
- 96 quantification limit in the first time interval were not included.
- 97 2.2. Data collection
- 98 The kinetics were gathered from either the figures or the tables of the selected studies. 99 The digitize R package (23) was used to retrieve data from scatter plots in figures. This 100 package loads a graphical file of a scatterplot (in jpeg format) in the graphical window of 101 R and calibrates and extracts the data. Data were manually reported in R vector for data 102 provided in tables. A key was attributed to kinetics collected in each study (Table 1). The 103 specific list of tables and figures used for each kinetics is given in appendix 1.

104 2.3. Modelling of inactivation

105 A simple primary model was used for describing each inactivation kinetics. The D-values 106 (or decimal reduction times) were determined from the kinetics of the log_{10} number of 107 infectious viruses (*N*) over time at each experimental temperature. *D* is the inverse of 108 the slope of the inactivation kinetics.

109
$$log_{10}(N) = log_{10}(N_0) - t/D$$
 eq. (1)

Several secondary models describing the impact of temperature (T) and relative
humidity (RH) on *D* values were tested. The gamma concept of inactivation was used
(24, 25). In this approach, the inactivation of a microbial population could be estimated
by:

114
$$log_{10}(D) = log_{10}(D_{ref}) - \sum log_{10}(\lambda_{xi}(x_i))$$
 eq. (2)

115 Where λ_{xi} quantifies the influence of each environmental factors (x_i corresponds to

116 temperature and relative humidity in this study) on the microbial resistance (D_{ref})

117 observed in reference conditions.

Based on eq. (2), five different secondary models were established. Models #1, #2 and#3 do not consider the nature of the fomite.

- 120 Model #1 is the classical Bigelow model (26). It models only the effect of temperature.
- 121 The z_T , the increase of temperature which leads to a tenfold reduction of D, value was
- 122 determined as the negative inverse slope of the plot of $log_{10}(D)$ versus temperature. z_T is
- 123 the increase of temperature which leads to a ten-fold reduction of the decimal reduction

124 time. T_{ref} is the reference temperature (set to 4°C in our study) and $log_{10}(D_{ref})$ is the

125
$$\log_{10}(D)$$
 at T_{ref}

126 Model #1

127
$$log_{10}(\lambda_T(T)) = \frac{T - T_{ref}}{z}$$
 and $log_{10}(\lambda_{RH}(RH)) = 0$

128 Model #2 considers the effect of temperature, however *D* values were fitted according to

129 temperature using a semi-log approach, derived from Mafart (25).

130
$$log_{10}(\lambda_T(T)) = \left(\frac{T-T_{ref}}{Z_T}\right)^2$$
 and $log_{10}(\lambda_{RH}(RH)) = 0$

131 Model #3 is similar to model #2 but the shape parameter *n* was estimated instead of

132 being set to 2.

133
$$log_{10}(\lambda_T(T)) = \left(\frac{T-T_{ref}}{Z_T}\right)^n$$
 and $log_{10}(\lambda_{RH}(RH)) = 0$

The last two models (#4 and #5) consider the effect of temperature and the nature of the fomites. The type of fomite was taken into account through the use of relative humidity. Suspensions correspond to more than 99% RH conditions while surfaces are associated with RH conditions below to this threshold. The models consider that surfaces at higher relative humidity allow for more rapid inactivation and that inactivation in suspensions is equivalent to inactivation on surfaces exposed to low RH. In model #4, the shape

141 parameter for temperature was set to 2 as in model #2.

142
$$log_{10}(\lambda_T(T)) = \left(\frac{T - T_{ref}}{Z_T}\right)^2$$
 and $log_{10}(\lambda_{RH}(RH)) = \begin{cases} \frac{RH}{Z_{RH}} & RH < 99\% \\ 0 & RH \ge 99\% \end{cases}$

143 In model #5, n is a model parameter to be estimated.

144
$$log_{10}(\lambda_T(T)) = \left(\frac{T-T_{ref}}{Z_T}\right)^n$$
 and $log_{10}(\lambda_{RH}(RH)) = \begin{cases} \frac{RH}{Z_{RH}} & RH < 99\% \\ 0 & RH \ge 99\% \end{cases}$

145 In models #4 and #5, z_{RH} is the increase of relative humidity, which leads to a ten-fold 146 reduction of the decimal reduction time.

147 2.4. Model's parameters estimation

The model's parameters were fitted with nls() R function. Confidence intervals of fitted
parameters were assessed by bootstrap using nlsBoot() function from nlsMicrobio R
package (27). The five models were compared according to penalized-likelihood criteria,
the Aikaike information criterion (AIC) (28) and Bayesian information criterion (BIC) (29).

$$AIC = p.Ln\left(\frac{RSS}{p}\right) + 2k$$

$$BIC = p.Ln\left(\frac{RSS}{p}\right) + k.Ln(p)$$

Where RSS is the residual sum of squares, *p* is the number of experimental points and *k*the number of parameters in the model. The lower the AIC and BIC, the better the model
fits the dataset.

155 2.5. Data availability

The detailed information on the tables and figures where the data were collected are
given in appendix 1. All the scripts and data used to prepare figures and tables of this
manuscript are available in a Github repository (30).

159

160 3. Results

161 3.1. Literature review results

162 Table 1 shows the detailed characteristics of the twenty-six studies that characterized 163 inactivation of a virus from the Coronaviridae family according to temperature and or 164 relative humidity. Some kinetics were not appropriate for characterizing inactivation rate 165 either because the duration of the experiments was too short to observe any significant 166 decrease of virus infectivity, or because the quantification limit was reached before the 167 first time point (Table 1). A total of 102 estimates of D-value were collected from 25 of 168 the 26 studies (Appendix 1). These kinetic values represent 605 individual data points. 169 For each curve, a D-value (i.e. decimal reduction time) was estimated. The 102 D-values 170 are given in Appendix 1. Among the 102 kinetic values, 44 are from members of the 171 Alphacoronavirus genus including one from Canine coronavirus (CCV), two for the feline 172 infectious peritonitis virus (FIPV), five for the porcine epidemic diarrhea virus (PEDV), 14 173 for the Human coronavirus 229E (HCoV-229E) and 22 from the porcine transmissible 174 gastroenteritis coronavirus (TGEV). The remaining 58 kinetics are related to the

Betacoronavirus genus, including two Human coronavirus - OC43 (HCoV-OC43), two for
the bovine coronavirus, 13 for the murine hepatitis virus (MHV), eight for the MERSCoV, 22 for the SARS-CoV and 11 for the SARS-CoV-2. Figure 1 shows the 102
estimates of D-values, including 40 values on inert surfaces and 62 values in
suspension from temperatures ranging from 4°C to 68°C. Different suspensions were
noted, but most were laboratory media (Table 1).

181 **3.2. Modelling the inactivation**

182 The 102 D-values were fitted with five different models. Table 2 shows the performance 183 of these models to describe D-values according to temperature and relative humidity. 184 For the tested range of temperatures (between 4 and 68°C), model #1 (the classical 185 Bigelow model) based on a log-linear relation between D-values and temperature does 186 not perform as well as model #2 that considers a linear second-degree equation. Model 187 #3 offers a further refinement over model #2 by also fitting the degree of the equation (n188 parameter). The fitted value of n was equal to 1.9 with a confidence interval that 189 includes 2 (*i.e.* model #2). Accordingly, the values taken by the parsimony criterions for 190 model selection AIC and BIC for model #2 and #3, indicate that *n* can be set to 2. 191 Figure 2 illustrates the performance of models #1 (Fig. 2A), #2 (Fig. 2B) and #3 (Fig. 3C) 192 for which only temperature effect is considered for predicting D-values. 193 Table 2 demonstrates that the inclusion of relative humidity should be considered. 194 Models #4 and #5 that describe the D-values according to temperature and relative 195 humidity were more appropriate models than models #1, #2 and #3 with a decrease of 196 AIC of more than 2 points in comparison with other models (31). The estimated value for 197 the shape parameter in model #5 is not different from the value two. According to BIC

198 criterion, model #4 and model #2 were the most appropriate and undistinguishable. 199 Based on these comparisons, model #4 was retained. Figure 3A shows the prediction of 200 inactivation rate according to T and RH for this model. The high z_{RH} value (Table 2) 201 indicates that the impact of RH is far less important than temperature. For example, 202 increasing the relative humidity by 80%, e.g. from 10% to 90%, only reduces the D 203 values by a factor of 1.7. The same reduction factor of D-values can be obtained by a 204 small change of temperature, (e.g. changing from 10 to 15°C or from 60 to 61°C). Model 205 #2 was retained as well as it provides very similar performance. Figures 3B shows the 206 residuals for model #4. Comparative analysis of residuals of models #2 and #4 are 207 provided in Appendix 2 (Figure A2-1).

208

209 3.3. Potential use of the model

210 An Excel spreadsheet implementing model #4 has been prepared and is available in 211 Appendix 3. The spreadsheet can be used to estimate the number of decimal reductions 212 of infectivity of coronaviruses according to user defined time, temperature and relative 213 humidity. For example, the predicted inactivation at a temperature of 70°C for 1 minute 214 in liquid is -11.8 log₁₀ with a 95% CI [-6.4; -22.1] for model #4 and -11.1 log₁₀ with a 215 95% CI [-5.7; -21.4] for model #2. The spreadsheet also allows an estimate of the time 216 necessary to reach a target number of decimal reductions of infectivity with a certain 217 confidence level for both model #4 and model #2. For example, the time to reach a 5 218 log₁₀ inactivation at 20°C and 75% relative humidity is 304 h with a 95% CI of [215; 426]. 219 It will be much longer at 20% relative humidity as the time to reach a 5 log₁₀ inactivation 220 is predicted to be 438 h with a 95% CI of [339; 569]. Model #2 (that does not take into

account relative humidity), provides an estimate of the time to reach a 5 log₁₀

222 inactivation at 20°C of 412 h with a 95% CI of [322; 539].

223

224 4. Discussion

Our study identified 102 kinetic values for inactivation of coronaviruses on surfaces and in suspensions. The included studies cover those identified in three recently published articles that conducted a systematic review on coronaviruses inactivation (32-34). These data were used to suggest a novel inactivation model specific to the *Coronaviridae* family. The modelling approach identified temperature and relative humidity as major

230 factors needed to predict infectious coronavirus persistence on fomites.

231 The log₁₀ of D values was not linearly related to temperature in the range of 232 temperatures studied (4 – 68° C). Bertrand et al. (15) made a similar observation in a 233 meta-analysis for virus and phage inactivation in foods and water and proposed two 234 different models on either side of the threshold temperature of 50°C. Laude (16) 235 suggested a similar approach for TGEV with a threshold temperature at 45°C (16). The 236 modelling approach we used in our study allows fitting the inactivation values with a 237 single relation. In other meta-analysis on inactivation of viruses, Boehm et al. (22) and 238 Heßling et al. (35) did not observe such different trends but also studied smaller 239 temperature ranges. In the highest range of temperature (above 60°C), coronaviruses 240 are found to be far less heat resistant than non-enveloped viruses (36).

241 The present modelling approach considers the non-monotonous impact of relative

242 humidity on inactivation. Coronaviruses persisted better at low RHs and at 100% RH,

243 than for intermediate RHs. Another study has confirmed that low RH makes viruses

244 more resistant to thermal inactivation (37). Lin and Marr (38) recently observed the 245 same relation for two bacteriophages, where the observed RH where survival was worst 246 is close to 80% while in the present study, the less favorable condition for coronaviruses 247 was set to 99%. The data collected in the present study do not cover a uniform 248 distribution of temperatures and RH values. Further data corresponding to inactivation of 249 coronaviruses on surfaces at low humidities for temperature between 40 and 60°C 250 would help to refine assessment of impact of RH. Using a worst-case RH set to 99% 251 may be appropriate to estimate reductions in those situations until the model can be 252 refined. 253 As noted in the methods, all the kinetic values analyzed were established based on the 254 quantification of coronavirus infectivity with cell cultures. The model prediction did not 255 include other inactivation results from methods combining dyes with RT-qPCR. This 256 method (although more appropriate than classical RT-qPCR) can underestimate virus 257 infectivity (21, 22). 258 The data collected from the literature does not permit models specific to species at this 259 time. Our findings suggest that persistence potential of different coronaviruses is similar. 260 It confirms previous finding that advocates for the use of surrogates' coronavirus such 261 as TGEV (39). This could considerably simplify the acquisition of relevant data for 262 persistence potential for other environmental factors. The data analyzed here only 263 include Alpha- and Betacoronavirus, as no data for the two other major genera, Delta-

and *Gammacoronavirus*, were identified. Inclusion of such data would help to challengethe present model robustness.

266 The models developed in our study are specific to viruses from the *Coronaviridae* family.

267 Several studies on the inactivation of other viruses have suggested that the impact of

268 temperature can be modelled, as a whole, with a unique parameter (15, 22, 40). 269 Variability of behavior by virus type has been observed and model parameters to 270 account these differences have been proposed (22, 40), e.g. non-enveloped viruses are 271 known to show greater persistence in the environment (40). Like a recently proposed 272 model for SARS-CoV-2 (41), our model takes into consideration of relative humidity in 273 the prediction of inactivation. This integration is of high interest in the perspective of 274 assessment of seasonality on virus persistence (42). 275 It's also worth noting our model is specific to fomites. Survival kinetics in fecal materials 276 were identified (43) but not considered for inclusion. The level of matrix contamination 277 with fecal materials has been shown to significantly increase the inactivation rate of 278 viruses (40), so by excluding these data, model predictions are biased to be fail-safe. 279 Inactivation data on porous surfaces were also not considered since it may be difficult to 280 determine if any measured inactivation is associated with real loss of infectivity or 281 difficulty in recovering viruses absorbed inside the porous material. That said, there is no 282 reason to consider that model predictions for coronaviruses are not pertinent to survival 283 on porous material (e.g. face masks). 284 Inactivation on anti-microbial surfaces, such as copper and silver, was also not 285 considered. For the same reason, model predictions are fail safe as surfaces including 286 copper or other antimicrobial compounds increase the inactivation rate of coronaviruses 287 (12, 44). 288 The predictions of the present model could support more robust decision-making and 289 could be useful in various contexts such as blood safety assessment (45) or validation of 290 thermal inactivating treatments for room air, surfaces or suspensions. Indeed, an 291 important issue is the possibility of reusing privates or public offices, rooms of hotels, or

292 vehicles that are difficult to decontaminate. Moreover, many devices like electronics or 293 more sensitive materials, are not suitable for chemical decontamination processes which 294 could make them inoperative. Another aspect of decontamination is the economical 295 challenge as large scale decontamination of buildings can cost billions of dollars (46). 296 Furthermore, the use of detergents and/or disinfectants may have environmental 297 consequences. Thus the large scale decontamination of surfaces for SARS-CoV-2 that 298 are not necessarily in contact with people may not be required. For these reasons the 299 waiting time needed before handling suspected contaminated materials in absence of 300 decontamination is more than ever an important question. Having a calculator for the 301 natural clearance of SARS-CoV-2 depending on temperature could be a valuable 302 operational tool for public authorities (41). 303 The present model also opens the way for risk assessment for SARS-CoV-2 304 transmission through contact (47). Further model developments including data on matrix 305 pH, salinity and exposure to visible and UV light would also be important to consider (40, 306 48).

307 5. Acknowledgements

308 The Covid-19 Emergency Collective Expert Appraisal Group members included the co-

309 authors LG, S.M-L, E.C, N.P, S.L.P, M.S. and (in alphabetical order): Paul Brown,

310 Charlotte Dunoyer, Florence Etore, Elissa Khamisse, Meriadeg Legouil, François

- 311 Meurens, Gilles Meyer, Elodie Monchatre-Leroy, Gaëlle Simon and Astrid Vabret.
- 312
- 313
- 314

315 6. References

- Kutter JS, Spronken MI, Fraaij PL, Fouchier RA, Herfst S. 2018. Transmission routes of respiratory viruses among humans. Current Opinion in Virology 28:142-151.
- Lu J, Gu J, Li K, Xu C, Su W, Lai Z, Zhou D, Yu C, Xu B, Yang Z. 2020. COVID Outbreak associated with air conditioning in restaurant, Guangzhou, China,
 Emerging Infectious Diseases 26.
- Lee N, Hui D, Wu A, Chan P, Cameron P, Joynt GM, Ahuja A, Yung MY, Leung
 C, To K. 2003. A major outbreak of severe acute respiratory syndrome in Hong
 Kong. New England Journal of Medicine 348:1986-1994.
- Kim S-H, Chang SY, Sung M, Park JH, Bin Kim H, Lee H, Choi J-P, Choi WS, Min J-Y. 2016. Extensive viable Middle East respiratory syndrome (MERS) coronavirus contamination in air and surrounding environment in MERS isolation wards. Reviews of Infectious Diseases 63:363-369.
- Liu J, Liao X, Qian S, Yuan J, Wang F, Liu Y, Wang Z, Wang F, Liu L, Zhang Z.
 Community transmission of Severe Acute Respiratory Syndrome
 Coronavirus 2, Shenzhen, China, 2020. Emerging Infectious Diseases 26.
- 6. Chen Y-C, Huang L-M, Chan C-C, Su C-P, Chang S-C, Chang Y-Y, Chen M-L,
 Hung C-C, Chen W-J, Lin F-Y. 2004. SARS in hospital emergency room.
 Emerging Infectious Diseases 10:782.
- 7. Danis K, Epaulard O, Bénet T, Gaymard A, Campoy S, Bothelo-Nevers E, Bouscambert-Duchamp M, Spaccaferri G, Ader F, Mailles A, Boudalaa Z, Tolsma V, Berra J, Vaux S, Forestier E, Landelle C, Fougere E, Thabuis A, Berthelot P, Veil R, Levy-Bruhl D, Chidiac C, Lina B, Coignard B, Saura C, Team I. 2020.
 Cluster of coronavirus disease 2019 (Covid-19) in the French Alps, 2020. Clinical Infectious Diseases doi:10.1093/cid/ciaa424.
- Otter JA, Donskey C, Yezli S, Douthwaite S, Goldenberg SD, Weber DJ. 2016.
 Transmission of SARS and MERS coronaviruses and influenza virus in healthcare settings: the possible role of dry surface contamination. Journal of Hospital Infection 92:235-250.
- Wolff MH, Sattar SA, Adegbunrin O, Tetro J. 2005. Environmental survival and
 microbicide inactivation of coronaviruses, p 201-212, Coronaviruses with special
 emphasis on first insights concerning SARS. Springer.
- 34810.Medema G, Heijnen L, Elsinga G, Italiaander R, Brouwer A. 2020. Presence of349SARS-Coronavirus-2insewage.medRxiv350doi:https://doi.org/10.1101/2020.03.29.20045880.
- 11. Chin A, Chu J, Perera M, Hui K, Yen H-L, Chan M, Peiris M, Poon L. 2020.
 Stability of SARS-CoV-2 in different environmental conditions. The Lancet
 Microbe https://doi.org/10.1016/S2666-5247(20)30003-3.
- van Doremalen N, Bushmaker T, Morris DH, Holbrook MG, Gamble A, Williamson
 BN, Tamin A, Harcourt JL, Thornburg NJ, Gerber SI. 2020. Aerosol and surface
 stability of SARS-CoV-2 as compared with SARS-CoV-1. New England Journal of
 Medicine.
- Casanova LM, Jeon S, Rutala WA, Weber DJ, Sobsey MD. 2010. Effects of air
 temperature and relative humidity on coronavirus survival on surfaces. Appl
 Environ Microbiol 76:2712-2717.

- 361 14. Bozkurt H, D'Souza DH, Davidson PM. 2015. Thermal inactivation kinetics of human norovirus surrogates and hepatitis A virus in turkey deli meat. Appl Environ Microbiol 81:4850-4859.
- Bertrand I, Schijven J, Sánchez G, Wyn-Jones P, Ottoson J, Morin T, Muscillo M,
 Verani M, Nasser A, de Roda Husman A. 2012. The impact of temperature on the
 inactivation of enteric viruses in food and water: a review. Journal of Applied
 Microbiology 112:1059-1074.
- Laude H. 1981. Thermal inactivation studies of a coronavirus, transmissible
 gastroenteritis virus. Journal of General Virology 56:235-240.
- Van Doremalen N, Bushmaker T, Munster V. 2013. Stability of Middle East
 respiratory syndrome coronavirus (MERS-CoV) under different environmental
 conditions. Eurosurveillance 18:20590.
- Ijaz M, Brunner A, Sattar S, Nair RC, Johnson-Lussenburg C. 1985. Survival characteristics of airborne human coronavirus 229E. Journal of General Virology 66:2743-2748.
- Ijaz M, Karim Y, Sattar S, Johnson-Lussenburg C. 1987. Development of
 methods to study the survival of airborne viruses. Journal of Virological Methods
 18:87-106.
- Rabenau H, Cinatl J, Morgenstern B, Bauer G, Preiser W, Doerr H. 2005. Stability
 and inactivation of SARS coronavirus. Medical Microbiology and Immunology
 194:1-6.
- Coudray-Meunier C, Fraisse A, Martin-Latil S, Guillier L, Perelle S. 2013.
 Discrimination of infectious hepatitis A virus and rotavirus by combining dyes and surfactants with RT-qPCR. BMC microbiology 13:216.
- Boehm AB, Silverman AI, Schriewer A, Goodwin K. 2019. Systematic review and
 meta-analysis of decay rates of waterborne mammalian viruses and coliphages in
 surface waters. Water research 164:114898.
- Poisot T. 2011. The digitize package: extracting numerical data from scatterplots.
 The R Journal 3:25-26.
- Coroller L, Kan-King-Yu D, Leguerinel I, Mafart P, Membré J-M. 2012. Modelling
 of growth, growth/no-growth interface and nonthermal inactivation areas of
 Listeria in foods. International Journal of Food Microbiology 152:139-152.
- Mafart P. 2000. Taking injuries of surviving bacteria into account for optimising
 heat treatments. International Journal of Food Microbiology 55:175-179.
- Bigelow W. 1921. The logarithmic nature of thermal death time curves. The
 Journal of Infectious Diseases:528-536.
- Baty F, Delignette-Muller M. 2017. nlsMicrobio: data sets and nonlinear
 regression models dedicated to predictive microbiology. R package version 0.0-1.
- Akaike H. 1974. A new look at the statistical model identification. IEEE
 Transactions on Automatic Control 19:716-723.
- 401 29. Schwarz G. 1978. Estimating the dimension of a model. The Annals of Statistics
 402 6:461-464.
- 40330.Guillier L. 2020. Data and models related to coronaviruses inactivation.404https://github.com/lguillier/Persistence-Coronavirus.
- 405 31. Burnham KP, Anderson DR. 1998. Practical use of the information-theoretic 406 approach, p 75-117, Model selection and inference. Springer.

407 32. Kampf G, Voss A, Scheithauer S. 2020. Inactivation of coronaviruses by heat.
408 Journal of Hospital Infection.

- 409 33. La Rosa G, Bonadonna L, Lucentini L, Kenmoe S, Suffredini E. 2020.
 410 Coronavirus in water environments: Occurrence, persistence and concentration 411 methods-A scoping review. Water Research:115899.
- 412 34. Kampf G, Todt D, Pfaender S, Steinmann E. 2020. Persistence of coronaviruses
 413 on inanimate surfaces and its inactivation with biocidal agents. Journal of Hospital
 414 Infection.
- 415 35. Heßling M, Hoenes K, Lingenfelder C. 2020. Selection of parameters for thermal
 416 Coronavirus inactivation–A data-based recommendation. GMS Hygiene and
 417 Infection Control in press.
- 418 36. Firquet S, Beaujard S, Lobert P-E, Sané F, Caloone D, Izard D, Hober D. 2014.
 419 Viruses contained in droplets applied on warmed surface are rapidly inactivated.
 420 Microbes and Environments 29:408-412.
- 421 37. Sauerbrei A, Wutzler P. 2009. Testing thermal resistance of viruses. Archives of virology 154:115-119.
- 423 38. Lin K, Marr LC. 2019. Humidity-Dependent Decay of Viruses, but Not Bacteria, in
 424 Aerosols and Droplets Follows Disinfection Kinetics. Environmental Science &
 425 Technology 54:1024-1032.
- 426 39. Casanova L, Rutala WA, Weber DJ, Sobsey MD. 2009. Survival of surrogate 427 coronaviruses in water. Water research 43:1893-1898.
- 428 40. Brainard J, Pond K, Hunter PR. 2017. Censored regression modeling to predict
 429 virus inactivation in wastewaters. Environmental science & technology 51:1795430 1801.
- 431 41. United States Department of Homeland Security. 2020. SARS-CoV-2 Indoor
 432 Environmental Stability Predictive Model. Available at:
 433 <u>https://www.dhs.gov/sites/default/files/publications/sars-cov-</u>
 434 2 environment predictive model factsheet 2.pdf
- 435 42. Prussin AJ, Schwake DO, Lin K, Gallagher DL, Buttling L, Marr LC. 2018.
 436 Survival of the enveloped virus Phi6 in droplets as a function of relative humidity, 437 absolute humidity, and temperature. Appl Environ Microbiol 84:e00551-18.
- 438 43. Lai MY, Cheng PK, Lim WW. 2005. Survival of severe acute respiratory 439 syndrome coronavirus. Clinical Infectious Diseases 41:e67-e71.
- 440 44. Warnes SL, Little ZR, Keevil CW. 2015. Human coronavirus 229E remains 441 infectious on common touch surface materials. MBio 6:e01697-15.
- 44245.Chang L, Yan Y, Wang L. 2020. Coronavirus Disease 2019: Coronaviruses and443BloodSafety.TransfusionMedicineReviews444doi:https://doi.org/10.1016/j.tmrv.2020.02.003.
- 445 46. Schmitt K, Zacchia NA. 2012. Total decontamination cost of the anthrax letter
 446 attacks. Biosecurity and bioterrorism: biodefense strategy, practice, and science
 447 10:98-107.
- 448 47. Haas C. 2020. Coronavirus and Risk Analysis. Risk Analysis 40:660-661.
- 449 48. Heßling M, Hönes K, Vatter P, Lingenfelder C. 2020. Ultraviolet irradiation doses
 450 for coronavirus inactivation–review and analysis of coronavirus photoinactivation
 451 studies. GMS Hygiene and Infection Control 15.

- 49. Mullis L, Saif LJ, Zhang Y, Zhang X, Azevedo MS. 2012. Stability of bovine
 453 coronavirus on lettuce surfaces under household refrigeration conditions. Food
 454 Microbiology 30:180-186.
- 455 50. Saknimit M, Inatsuki I, Sugiyama Y, Yagami K. 1988. Virucidal efficacy of
 456 physico-chemical treatments against coronaviruses and parvoviruses of
 457 laboratory animals. Jikken dobutsu Experimental animals 37:341.
- 458 51. Christianson K, Ingersoll J, Landon R, Pfeiffer N, Gerber J. 1989.
 459 Characterization of a temperature sensitive feline infectious peritonitis 460 coronavirus. Archives of Virology 109:185-196.
- 461 52. Gundy PM, Gerba CP, Pepper IL. 2009. Survival of coronaviruses in water and 462 wastewater. Food and Environmental Virology 1:10.
- 463 53. Bucknall RA, King LM, Kapikian AZ, Chanock RM. 1972. Studies with human coronaviruses II. Some properties of strains 229E and OC43. Proceedings of the Society for Experimental Biology and Medicine 139:722-727.
- 466 54. Sizun J, Yu M, Talbot P. 2000. Survival of human coronaviruses 229E and OC43
 467 in suspension and after drying onsurfaces: a possible source of hospital-acquired
 468 infections. Journal of Hospital Infection 46:55-60.
- 469 55. Lamarre A, Talbot PJ. 1989. Effect of pH and temperature on the infectivity of 470 human coronavirus 229E. Canadian Journal of Microbiology 35:972-974.
- 471 56. Leclercq I, Batejat C, Burguière AM, Manuguerra JC. 2014. Heat inactivation of
 472 the Middle East Respiratory Syndrome coronavirus. Influenza and Other
 473 Respiratory Viruses 8:585-586.
- 474 57. Ye Y, Ellenberg RM, Graham KE, Wigginton KR. 2016. Survivability, partitioning,
 475 and recovery of enveloped viruses in untreated municipal wastewater.
 476 Environmental Science & Technology 50:5077-5085.
- 477 58. Hofmann M, Wyler R. 1989. Quantitation, biological and physicochemical properties of cell culture-adapted porcine epidemic diarrhea coronavirus (PEDV).
 479 Veterinary Microbiology 20:131-142.
- 480 59. Quist-Rybachuk G, Nauwynck H, Kalmar I. 2015. Sensitivity of porcine epidemic diarrhea virus (PEDV) to pH and heat treatment in the presence or absence of porcine plasma. Veterinary microbiology 181:283-288.
- Hulst MM, Heres L, Hakze-van der Honing R, Pelser M, Fox M, van der Poel WH.
 Study on inactivation of porcine epidemic diarrhoea virus, porcine
 sapelovirus 1 and adenovirus in the production and storage of laboratory spraydried porcine plasma. Journal of Applied Microbiology 126:1931-1943.
- 487 61. Darnell ME, Subbarao K, Feinstone SM, Taylor DR. 2004. Inactivation of the
 488 coronavirus that induces severe acute respiratory syndrome, SARS-CoV. Journal
 489 of virological methods 121:85-91.
- 490 62. Chan K, Peiris J, Lam S, Poon L, Yuen K, Seto W. 2011. The effects of
 491 temperature and relative humidity on the viability of the SARS coronavirus.
 492 Advances in Virology 2011.
- 493 63. Pagat A-M, Seux-Goepfert R, Lutsch C, Lecouturier V, Saluzzo J-F, Kusters IC.
 494 2007. Evaluation of SARS-Coronavirus decontamination procedures. Applied
 495 Biosafety 12:100-108.
- 496 64. Kariwa H, Fujii N, Takashima I. 2006. Inactivation of SARS coronavirus by means
 497 of povidone-iodine, physical conditions and chemical reagents. Dermatology
 498 212:119-123.

49965.Batejat C, Grassin Q, Manuguerra J-C, Leclercq I. 2020. Heat inactivation of the500SevereAcuteRespiratorySyndromeCoronavirus2.501bioRxiv:https://doi.org/10.1101/2020.05.01.067769.

Virus	Genus	Sub-genus	Strain	Measurement	Temperatures (°C)	Conditions associated with treatment	Study reference
BCoV	Betacoronavirus	Embecovirus	Strain 88	PFU in Human rectal tumor (HRT)-18 cells	4	Salad, Minimal Essential Media (MEM) containing 2% Fetal Bovine Serum (FBS)	(49)
ссу	Alphacoronavirus	Tegacovirus	I-71	CRFK cells (PFU)	60, 80 ^ª	MEM containing 2% Fetal Calf Serum (FCS)	(50)
FIPV	Alphacoronavirus	Tegacovirus	DF2-WT	Feline kidney (NLFK) cells	54	Basal Medium Eagle	(51)
FIPV	Alphacoronavirus	Tegacovirus	ATCC-990	Crandell Reese feline kidney cell line	4 ^b , 23	Dechlorinated, filtered tap water	(52)
HCoV	Alphacoronavirus	Duvinacovirus	229E	Cellular infectivity in cell strain (HDCS) WI38	33, 37	Maintenance medium 2% FCS	(53)
HCoV	Alphacoronavirus	Duvinacovirus	229E	Cellular infectivity in lung cell line L132	21 ^b	PBS, Earle's MEM, Earle's MEM to with added suspended cells	(54)
HCoV	Alphacoronavirus	Duvinacovirus	229E	Cellular infectivity in lung cell line L132	21 ^b	Aluminum, sponge, latex at 65% RH	(54)
HCoV	Alphacoronavirus	Duvinacovirus	229E	CPE on MRC-5 cells	21	Teflon, PVC, Rubber, Steel, Plastic	(44)
HCoV	Alphacoronavirus	Duvinacovirus	229E	-	23	Cell culture supernatant with or without FBS	(20)
HCoV	Alphacoronavirus	Duvinacovirus	229E	MRC-5 cells (TCID-50)	4 ^b , 23	Dechlorinated, filtered tap water	(52)
HCoV	Alphacoronavirus	Duvinacovirus	229E	Cellular infectivity in lung cell line L132	4 ^b , 22, 33, 37	Earle's MEM	(55)
HCoV	Betacoronavirus	Embecovirus	OC43	Cellular infectivity in cell strain (HDCS) WI38	33, 37	Maintenance medium 2% FCS	(53)
HCoV	Betacoronavirus	Embecovirus	OC43	Cellular infectivity in human rectal tumor cell line HRT-18	21 ^b	PBS, Earle's MEM, Earle's MEM to with added suspended cells	(54)
HCoV	Betacoronavirus	Embecovirus	OC43	Cellular infectivity in human rectal tumor cell line HRT-18	21 ^b	Aluminum, sponge ^a , latex ^a at 65% RH	(54)
MERS-	Betacoronavirus	Sarbecovirus	FRA2	Cellular infectivity in	25 ^b , 56, 65	Cell culture supernatant	(56)

503 Table 1. Characteristics of the studies that explored inactivation of infectivity of coronavirus.

CoV				Vero cells (TCID-50)			
MERS- CoV	Betacoronavirus	Sarbecovirus	HCoV-EMC/2012	Cellular infectivity in Vero cells (TCID-50)	20, 30	Plastic (30%, 40% or 80% RH)	(17)
MERS- CoV	Betacoronavirus	Sarbecovirus	HCoV-EMC/2012	Cellular infectivity in Vero cells (TCID-50)	20, 30	Plastic (30%, 40% or 80% RH)	(17)
мну	Betacoronavirus	Embecovirus	-	Cellular infectivity in DBT cells	4 ^b , 25	Reagent-grade water	(39)
мну	Betacoronavirus	Embecovirus	-	Cellular infectivity in DBT cells	4 ^b , 25	Lake water	(39)
MHV	Betacoronavirus	Embecovirus	-	Cellular infectivity in DBT cells	4 ^b , 20, 40	Stainless steel surface with 20% humidity	(13)
MHV	Betacoronavirus	Embecovirus	-	Cellular infectivity in DBT cells	4, 20, 40	Stainless steel surface with 50% humidity	(13)
MHV	Betacoronavirus	Embecovirus	-	Cellular infectivity in DBT cells	4, 20, 40	Stainless steel surface with 80% humidity	(13)
мну	Betacoronavirus	Embecovirus	MHV-2	Cellular infectivity in DBT cells (PFU)	40 ^b , 60, 80 ^a	MEM containing 2% FCS	(50)
мну	Betacoronavirus	Embecovirus	MHV-N	Cellular infectivity in DBT cells (PFU)	40 ^b , 60, 80 ^a	MEM containing 2% FCS	(50)
MHV	Betacoronavirus	Embecovirus	A59	Plaque assay on L2 cells	10 ^b , 25	Pasteurized wastewater	(57)
PEDV	Alphacoronavirus	Pedacovirus	V215/78	PFU on Vero cells	50	Diluted medium for virus replication	(58)
PEDV	Alphacoronavirus	Pedacovirus	CV777	Vero cells (TCID-50)	40, 44, 48	MEM at pH 7.2	(59)
PEDV	Alphacoronavirus	Pedacovirus	CV777	Vero cells (TCID-50)	4 ^b , 44 ^b , 48	Medium at pH 7.5	(60)
SARS-CoV	Betacoronavirus	Sarbecovirus	FFM-1	Cellular infectivity in Vero cells	56	Cell culture supernatant with or without FBS	(20)
SARS-CoV	Betacoronavirus	Sarbecovirus	Urbani	Cellular infectivity in Vero cells	56, 65, and 75 ^a	Dulbecco's MEM	(61)
SARS-CoV	Betacoronavirus	Sarbecovirus	HKU39849	Cellular infectivity in FRH-K4 (TCID-50)	28, 33, 38	Plastic stored at 95% RH	(62)
SARS-CoV	Betacoronavirus	Sarbecovirus	HKU39849	Cellular infectivity in FRH-K4 (TCID-50)	28 ^b , 33, 38	Plastic stored at 80- 89% RH	(62)
SARS-CoV	Betacoronavirus	Sarbecovirus	GVU6109	Cellular infectivity in Vero cells (TCID-50)	20	Viral Transport Medium(VTM)	(43)
SARS-CoV	Betacoronavirus	Sarbecovirus	GVU6109	Cellular infectivity in Vero cells (TCID-50)	4, 20	Nasopharyngeal aspirate (NPA), throat and nasal swab (TNS)	(43)

						or VTM	
SARS-CoV	Betacoronavirus	Sarbecovirus	Tor2 AY274119.3	Cellular infectivity in Vero cells (TCID-50)	22	Plastic and stainless steel stored at 40°C	(12)
SARS-CoV	Betacoronavirus	Sarbecovirus	Utah	Cellular infectivity in Vero cells (TCID-50)	58, 68	Iscove's 4% FCS medium	(63)
SARS-CoV	Betacoronavirus	Sarbecovirus	Utah	Cellular infectivity in Vero cells (TCID-50)	22	Glass surface store at 10-25% RH	(63)
SARS-CoV	Betacoronavirus	Sarbecovirus	Hanoi	Cellular infectivity in Vero cells (TCID-50)	56	MEM	(64)
SARS- CoV2	Betacoronavirus	Sarbecovirus	-	Cellular infectivity in Vero cells (TCID-50)	4, 22, 37, 56, 70 ^a	VTM	(11)
SARS- CoV2	Betacoronavirus	Sarbecovirus	-	Cellular infectivity in Vero cells (TCID-50)	22	Plastic and stainless steel at 65% RH	(11)
SARS- CoV2	Betacoronavirus	Sarbecovirus	WA1-2020 (MN985325.1)	Cellular infectivity in Vero cells (TCID-50)	22	Plastic and stainless steel stored at 40°C	(12)
SARS- CoV2	Betacoronavirus	Sarbecovirus	-	Cellular infectivity in Vero cells (TCID-50)	56, 65 ^a	Cell culture supernatants	(65)
SARS- CoV2	Betacoronavirus	Sarbecovirus	-	Cellular infectivity in Vero cells (TCID-50)	65, 95 ^a	Nasopharyngal samples	(65)
SARS- CoV2	Betacoronavirus	Sarbecovirus	-	Cellular infectivity in Vero cells (TCID-50)	56	Sera	(65)
TGEV	Alphacoronavirus	Tegacovirus.	D52	Cellular infectivity in RPtg cells	31, 35, 39, 43, 47, 51 and 55	In HEPES solution at pH 7	(16)
TGEV	Alphacoronavirus	Tegacovirus.	D52	Cellular infectivity in RPtg cells	35, 39, 43, 47, and 51	In HEPES solution at pH 8	(16)
TGEV	Alphacoronavirus	Tegacovirus.	-	Cellular infectivity in ST cells	4 ^b , 20, 40	Stainless steel surface with 20% RH	(13)
TGEV	Alphacoronavirus	Tegacovirus.	-	Cellular infectivity in ST cells	4, 20, 40	Stainless steel surface with 50% RH	(13)
TGEV	Alphacoronavirus	Tegacovirus.	-	Cellular infectivity in ST cells	4, 20, 40	Stainless steel surface with 80% RH	(13)
TGEV	Alphacoronavirus	Tegacovirus.		Cellular infectivity in ST cells	4 ^b , 25	Reagent-grade water	(39)
TGEV	Alphacoronavirus	Tegacovirus.		Cellular infectivity in ST cells	4 ^b , 25	Lake water	(39)

^a not included: limit of quantification reached for the first sample time ^b not included: not enough decrease observed during experimentation - data not specified

505 506

507 Table 2. Characteristics of the different models fitted to the 102 decimal reduction time

508 data of coronaviruses according to temperature (T_{ref} set at 4°C) and relative humidity

Model	Fitted parameters	Best fit values [95%CI bootstrap intervals]	Bayesian information criterion	Aikaike information criterion
Model #1	log10Dref z _T	3.1 [2.8 - 3.3] 13.8 [12.7 - 15.1]	-124.7	-130.0
Model #2	log10Dref z _T	2.2 [2.1 - 2.3] 29.4 [28.4 - 30.5]	-160.6	-165.9
Model #3	log10Dref z⊤ n	2.3 [2.1 - 2.6] 27.7 [23.2 - 31.6] 1.9 [1.5 - 2.2]	-156.7	-164.6
Model #4	log10Dref z _T z _{RH}	2.3 [2.2 - 2.5] 29.1 [28.1 - 30.1] 341.4.7 [190.1 - 5631.4]	-160.2	-168.0
Model #5	log10Dref z _T z _{RH} n	2.4 [2.2 - 2.6] 27.5 [23.6 - 31.2] 330.7 [182.8 – 7020,1] 1.9 [1.6 - 2.2]	-156.2	-166.6

509

511

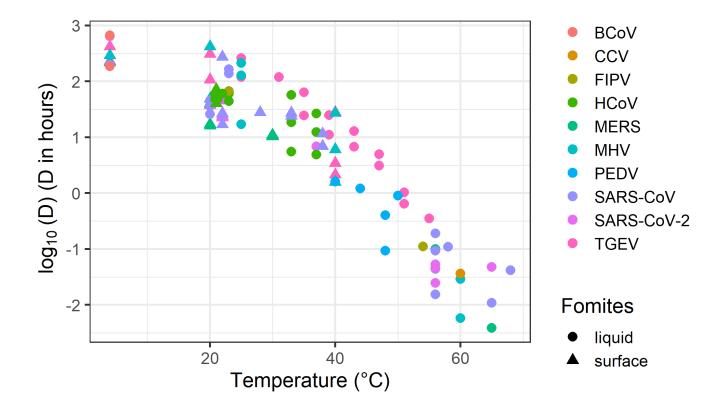
512	Figure 1. Decima	I reduction times	s of ten coronaviruse	es according to	temperature in
-----	------------------	-------------------	-----------------------	-----------------	----------------

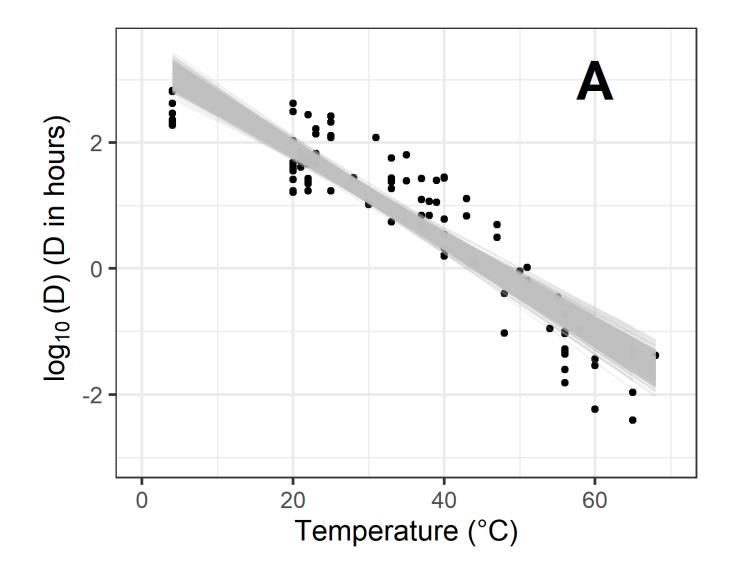
513 suspension or on inert surfaces.

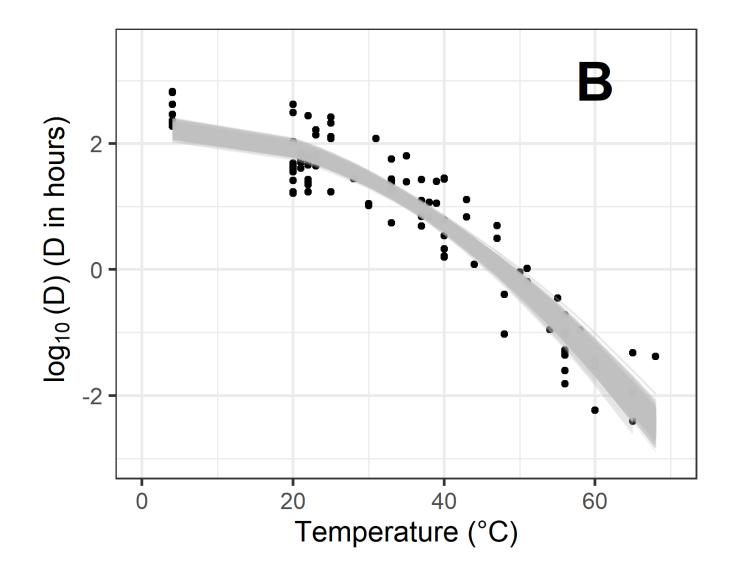
514

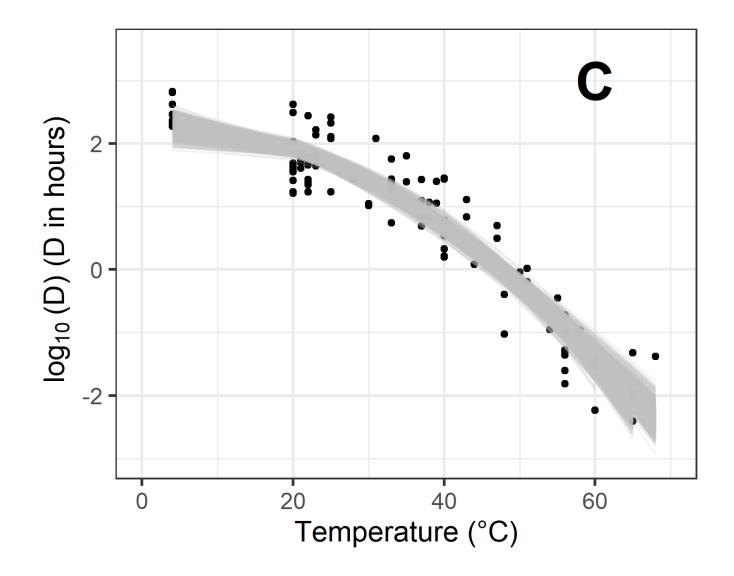
- 515 Figure 2. Observed (points) and fitted (grey lines) log decimal reduction time values
- 516 according to temperature for model #1 (A), model #2 (B) and #3 (C). One thousand (1000)
- 517 bootstrap values of uncertainty characterization are shown. Estimates of model
- 518 parameters are given in Table 2.

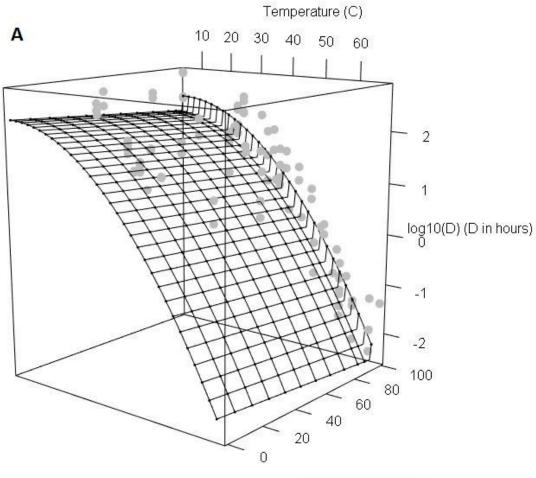
- 520 Figure 3. (A) Observed inactivation rate values (grey points) according to temperature
- 521 (°C) and relative humidity (%) and Model #4 surface predictions. Scatter points of
- 522 observed versus predicted D-values (D in hours) for model #4 (B). The dashed line
- 523 represents a perfect match between observations and predictions.











Relative Humidity (%)

